The evolution of a line echo wave pattern over the southern Taiwan area

Chih-Hsien Wei [1] 、Wen-Chau Lee [2] 、Tai-Hwa Hor [3] 、Mou-Hsiang Chang [4]

Department of Military Meteorology, Air force Institute of Technology [1]
National Center for Atmospheric Research [2]
General Education Center, Long Hua University [3]
Department of Atmospheric Science, National Taiwan University [4]

Abstract

A MCS developed over the southern part of the Taiwan Strait on 7 June 2003 (Fig 1). The leading convection possessed a LEWP moved through southern Taiwan and subsequently evolved into bow segments and MCVs. The northern part of the system was observed by both Central Weather Bureau's operational Doppler radars located at Chiku (RCCG) and Kenting (RCKT). Dual-Doppler wind synthesis from both radars thus can deduce the kinematic structure of the system. Not only it was a unique observation on LEWP, in subtropical area, but it is the first dual-Doppler observation of such a mesoscale system in East Asian area over the ocean to date. This paper presents the evolution and structure of this bow echo and MCV system particularly on the northern end of the system residing in the dual-Doppler lobe.

1. Introduction

Severe weather, such as downburst and tornado, can embed within a linear convective system that often possess concave or bulge segments on the plan position indicator (PPI) radar display. Nolen (1959) coined "line-echo-wave pattern (LEWP)" for this type of radar reflectivity pattern and linked LEWP to an episode of tornado. The LEWP may consist multiple bow-shaped radar echoes, which were named "bow echo" by Fujita (1978). Fujita also proposed a conceptual model of the bow echo evolution (Fig. 1) through many case studies observed over the continental United States.

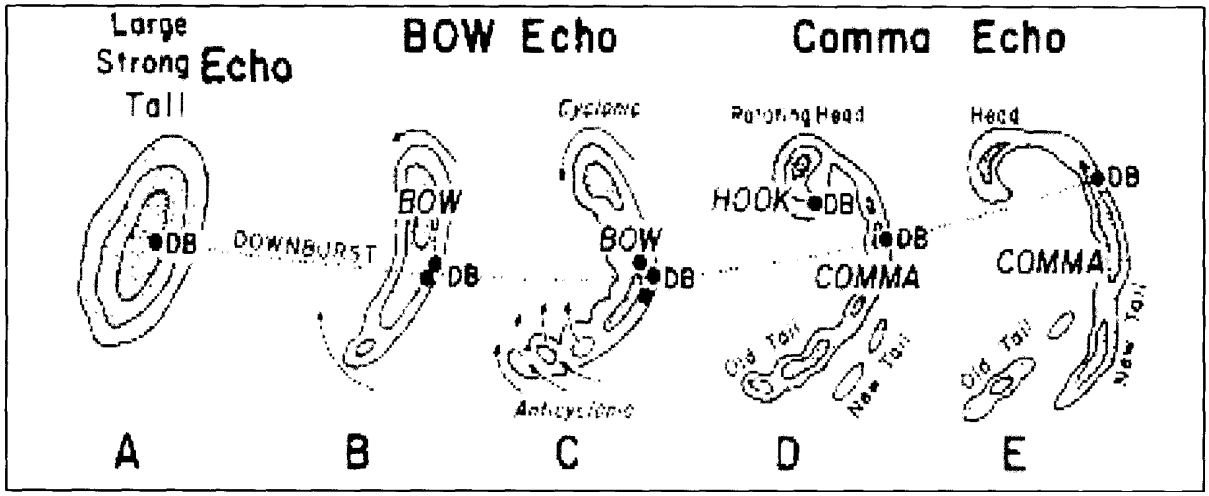

Fig.1 Schematic diagram of the evolution of a bow echo. (from Fujita 1978).

A bow echo is formed when a rear inflow jet developed behind the convective line and pushes the center part of the echo forward where downbursts might be in progress at this stage. It evolves into a comma-shape mesoscale convective vortex with a dominant cyclonic rotation near the head of the comma. Fujita also produced a first dual-Doppler analysis of a bow echo event during the Northern Illinois Meteorological Research on Downburst (NIMROD) and demonstrated the existence of a rear inflow jet behind the bulge of a bow echo (Fujita 1981).

Characteristics of bow echoes were examined by weather radar in 1980s. Przybylinski and Grey (1983) described that the presence of a channel of weak echo on the back side of a bow echo indicated the leading feature of a downburst event. Smull and Houze (1985; 1987) found that the weak echo channel is collocated with the rear-inflow jet (RIJ) which is a drier flow with ground-relative speed greater than 40 ms^{-1}. Burgee and Smull (1990) documented that a strong front to rear flow on both side of RIJ, indicating the existences of positive and negative vertical vorticity on both ends of the bow echo. Detection of these features may be connected to the initiation of severe wind events. Przybylinski (1995) identified the combination between weak echo channel and RIJ as "rear-inflow notch" (fig. 2) accordingly.

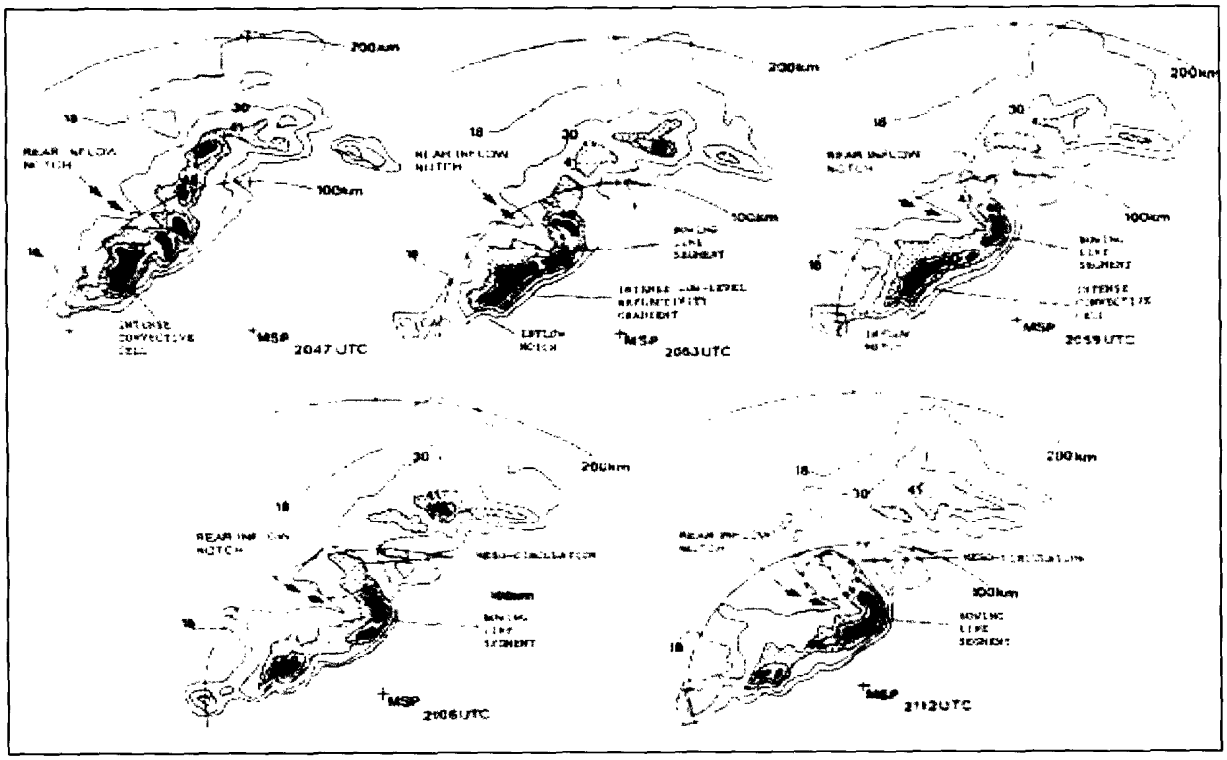

FIG.2 Radar analysis of the central Minnesota derecho between 2047 and 2112 UTC from Minneapolis–St. Paul, MN (MSP). Reflectivity contours are 18, 30, 41, and 46 dBZ. Shaded region represents reflectivity values greater than 50 dBZ. Arrow indicates the position of rear-inflow notch (From Przybylinski 1995).

Another useful radar signature typically linked to the onset of severe wind events is the mid-altitude radial convergence (MARC) signature (Schmocker 1996), which is defined as a region of strong radial convergence between the intense front-to-rear ascending updraft flow and the RIJ located in the transition region between 3 to 9 km in altitude. Przybylinski et al. (2000) found that initial bow echoes frequently developed near the intersection of a convective line and external boundary. By examining 273 bow echoes, Klimoski et al. (2004) traced the origins of these bow echoes to weak organized cells, squall lines and supercells and the bow echoes could grow upscale by thunderstorm merging process (fig. 3).

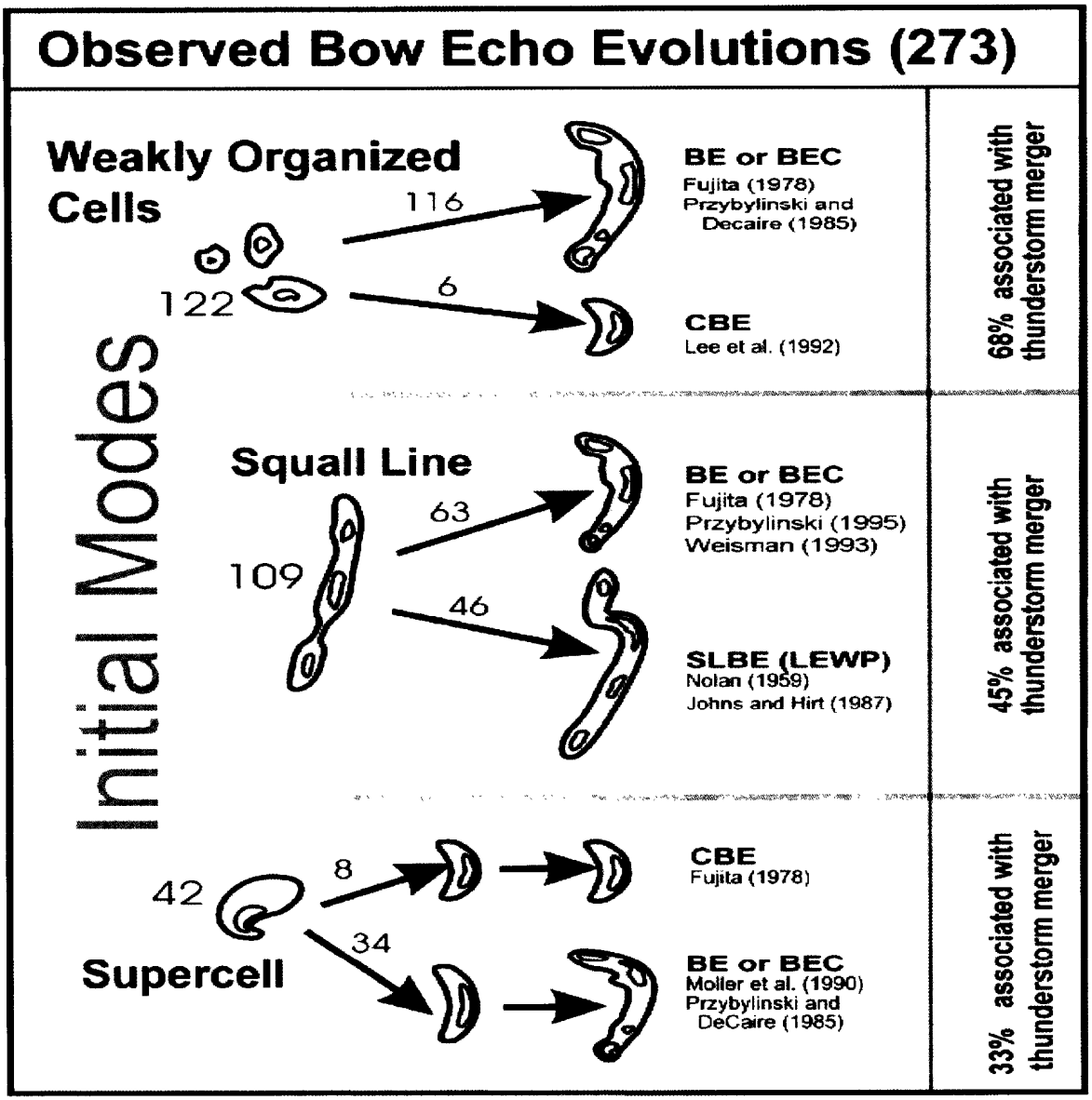

Fig.3 Illustration of the primary evolutionary pathways for bow echoes observed by Klimowski (2004). The number of cases identified following each path is indicated above the arrows. References for representative bow-echo cases are given. The percentage of bow echoes preceded by merging storms is given at right.

Our understanding of the bow echo evolution and the related environmental conditions has mostly been investigated by idealized numerical simulations. Weisman et al. (1988) presented that the environmental condition including a convective available potential energy (CAPE) value of 2400 J kg-1 and a unidirectional vertical wind shear of 25 ms-1 over the lowest 2.5 km AGL is favorable for the development of a quasi-linear convective system (QLCS). Weisman (1993) successfully simulated bow echoes embedded in QLCS and "bookend vortices" using similar environmental conditions. Weisman and Davis (1998) attribute the triggering mechanism of vortices to the vertical tilt of horizontal vorticity by the updraft along the gust front. The northern cyclonic vortex intensifies and becomes the dominated vortex by the midlevel convergence of planetary vorticity (Skamarock et al. 1994). Recent numerical simulations (Trapp and Weisman 2003; Weisman and Trapp 2003) suggested that some small scale straight-line wind damages often associated with bow echo events may be created by fast moving, small tornados where the ground-relative vortex velocity becomes asymmetric due to the storm motion.. However, the kinematic and dynamical structures of bow echoes and associated vortices have yet to be systematically sampled by multiple Doppler radars and dropwindsondes until the bow-echo and MCV experiment (BAMEX) in 2003 (Davis et al. 2004).

Even fewer bow echo events were observed/documented beyond the continental US.. During the Tropical Ocean Global Atmosphere Coupled Ocean-Atmosphere Research Experiment (TOGA COARE) a symmetric squall line evolved into a bow-shaped convective system which is documented by Jorgensen et al. (1997). The bow echo is characterized by a cyclonic vortex at its northern end and rear-inflow notch behind the intense echo, which are common for mid-latitude bow echoes. However, the CAPE was around 1440 J kg-1 and the environmental vertical wind shear was 13 ms-1 below 850 hPa, which is consistent with other tropical squall line environment but weaker than their mid-latitude counterparts. Businger et al. (1998) present an analysis for a bow echo associated with a subtropical low in the vicinity of Hawaii. They summarize a similar environmental condition for the development of a subtropical bow echo to the case occurred during TOCA COARE.

In Eastern Asia, the mesoscale convective systems (MCSs) developed along southeastern coast of China often propagate eastward over the Taiwan Strait where these systems could only be detected by satellite.. These MCSs are capable of producing heavy rainfall and occasional strong wind damages on the ground. Dual Doppler radar studies of several squall line systems propagating over the northern and central Taiwan during the Taiwan Area Mesoscale Experiment (TAMEX) in 1987 reveal that the dynamical structure of subtropical squall line resembles that of tropical squall line. However, these MCSs remain a challenge for both numerical models and forecasters due to insufficient observations in both the upstream environment and within the storm over the ocean. The completion of the around the island Doppler weather radar network in Taiwan in 2002 has provided the capability to monitor the evolution and

structures of these MCSs over the Taiwan Strait. More and more radar observations reveal these MCSs may exhibit QLCS with embedded bow-shaped segments.

This study documents the environment and single-Doppler characteristics of a LEWP event composed of several bow echo episodes observed from two Central Wather Bureau operational Doppler weather radars in Kenting and Chiku on 7 June 2003. It is believed that this is the first documentation of a LEWP system by Doppler radars over the subtropical, oceanic region in East Asia. These characteristics are compared with their counterparts in other part of the world. These LEWP systems and the potential for severe weathers do exist in East Asian and are threats to the safety in aviation and general publics. Mesoscale features and their comparisons with mid-latitude bow echoes describe in chapter 5. The evolution of associated mesovortices by using couplet signature of Doppler velocity presents in chapter 6. Another signature of LEWP will be proposed.

2. Data source

The Kenting (RCKT) and Chiku (RCCG) Doppler weather radar (fig. 4), which are constructed by Central weather Bureau (CWB), operated in 2001 and 2002, respectively. There are two scanning modes according to different ranges for both radars. The long distance scanning only including reflectivity field reach out to 460 km, and the range of Doppler scanning mode is 230 km. Other detailed information of both radars describe in table 1. The scanning interval for Kenting and Chiku radar per volume scan are 8 and 10 minute, respectively. In addition, Kenting radar does not execute data collecting within a deliberate sector on its northern side at lower elevations (below 2.4 degree), namely, the sector blanking strategy, so that avoid the influence of terrain. The collected radar data is transferred into universal format (UF, Barnes 1980) and then edited by implementing National Center for Atmospheric Research (NCAR) SOLO package. The NCAR REORDER software (Oye 1995) is applied for interpolating data into a Cartesian grid. Additional data sources include Geostationary Satellite-9 (GEOS-9) imageries and conventional observations which involve synoptic weather analyses, soundings and mesonet. Concerning less observation over the open ocean, synoptic reanalysis data from National Center for Environmental Prediction (NCEP) is an alternative for understanding the circumstances over the ocean.

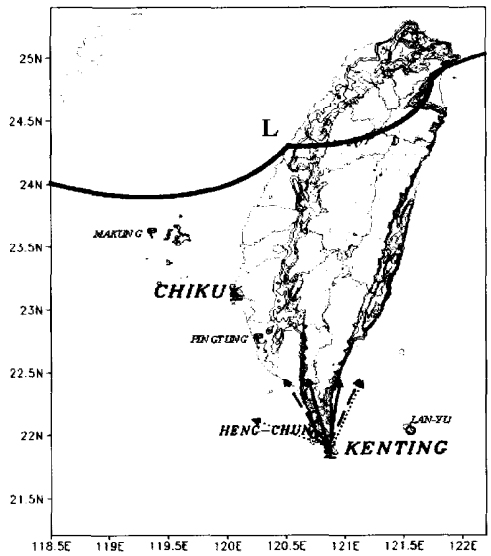

Fig.4 The observational area of this study. The symbol, Λ and **O** stands for weather radar site,sounding and surface observational stations,respectively.The intersecting angle between different types of arrow line onto Kenting radar represent sector blanking, including elevation of 0.5 (dot

line), 1.4 (long dash) and 2.4 (solid line). The position of surface front is also illustrated on the figure.

3. Description of Synoptic condition

A stationary front extended from northern Taiwan to southeastern coast of China at 0000 UTC 7 June (Fig. 5a). A wind shear line associated with a cyclonic circulation was approximately collocated with surface front below 850 hPa level (Fig. 5b). The horizontal temperature gradient (~1 °C per 100 km) was weak along the front, suggesting an imperceptible baroclinicity for prefrontal and postfrontal region. Meanwhile, the mesoscale surface analysis depicted that surface front was located between north and central Taiwan (fig. 4).

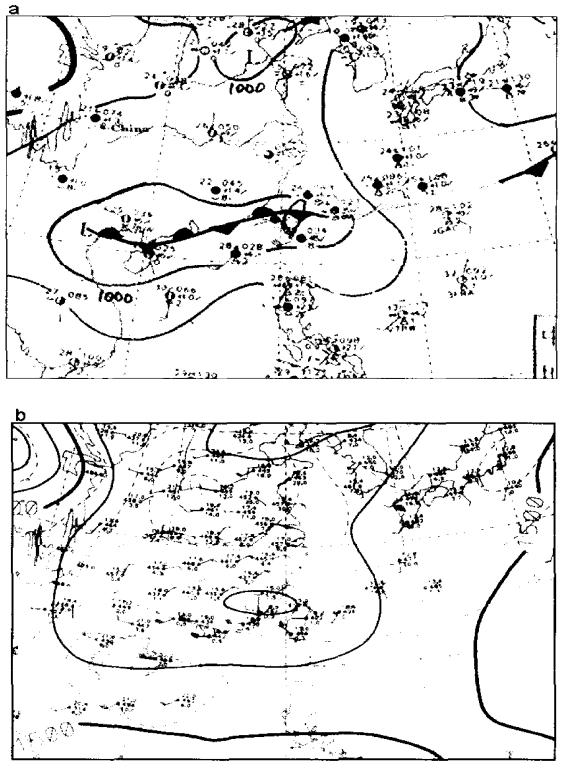

Fig.5 The weather chart at 0000 UTC 7 June 2003. (a) surface analysis. (b) upper analysis on 850 hPa. The island of Taiwan is enclosed by bold curve in (a). The dash line in (b) represents shear line at the level.

Therefore, the Makung (fig. 6a) and Pingtung (fig. 6b) sounding could represent the pre-frontal environment conditions. The CAPE calculated from both soundings were over 2000 J kg^{-1} at 1200 UTC (LST=UTC+8) 6 June and decreased to 700 kg^{-1} by 0000 UTC 7 June (only Makung sounding was available). At the same time the difference between dew point and air temperature was smaller than that at 1200 UTC 6 June, implying an adjustment by prior rainfall (do you have observational evidence of rain). Therefore, the environmental condition in southern Taiwan area was appropriate for development of convective rainband by 1200 UTC 6 June.

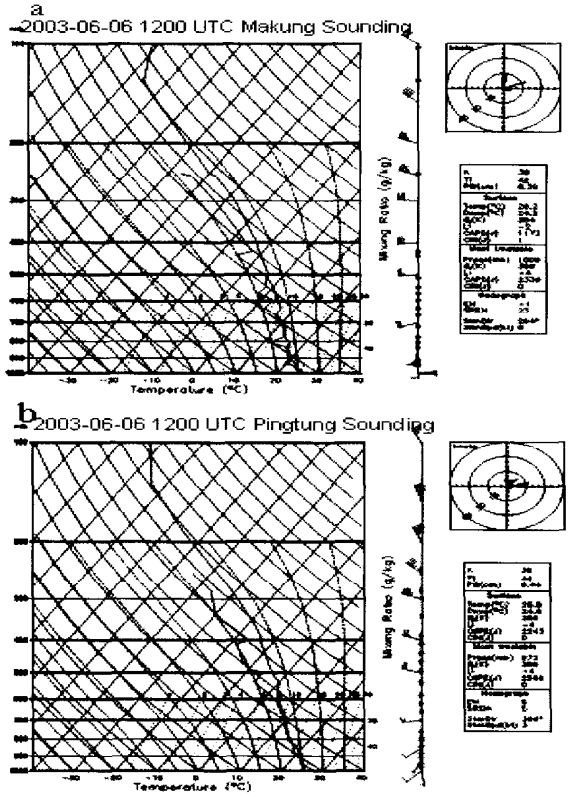

Fig.6 Skew-t diagrams from (a) Makung sounding and (b) Pingtung sounding at 1200 UTC 6 June 2003.

Besides, vertical wind shear below 700 hPa level was about 10 ms^{-1} estimated by Pingtung sounding at the same time and 15 ms^{-1} in the vicinity of developing region of the MCS by 0000 UTC 7 June (fig. 7). Comparing to previous research such as which Jorgensen et al. (1997) had documented, the bow-echo-type system occurred in tropical environment had a CAPE value of 1440 J kg^{-1} and vertical wind shear of 13 ms^{-1} at low level, which were not quite as severe as for midlatitude systems. However, the CAPE value in the present case was comparable with that in midlatitude counterpart. And the environmental vertical wind shear for the development of the MCS was similar to that for tropical squall line system.

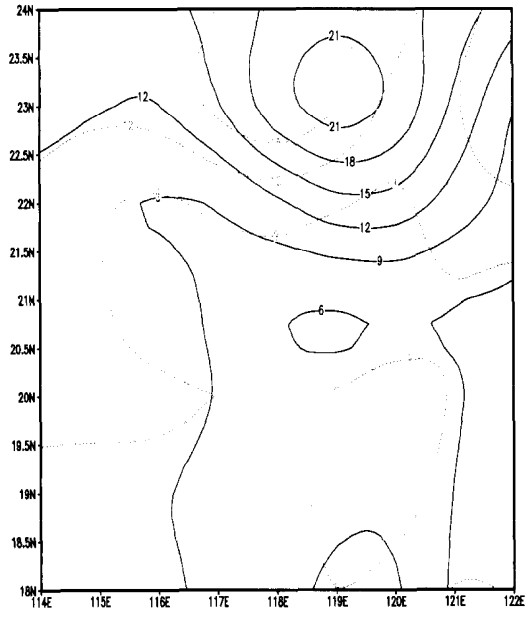

Fig.7 The vertical wind shear between 1000 and 700 hPa at 1800 UTC 6 June and 0000 UTC 7 June 2003. The unit of contour is ms-1.

The evolution of convective system.

By 0000 UTC 7 June 2003, a MCS developed over the southern Taiwan area extending into the southern Taiwan Strait, in which the GOES-9 satellite imagery (fig. 8) demonstrated that a belt of higher bright temperature split the system into two entities. The leading edge of western entity exhibited a curved line. The temperature on the cloud top of western portion was between -64 and -80 °C referring to color bar. According to the temperature profile of Makung sounding at the same time, the estimated height of cloud top was around 14 km.

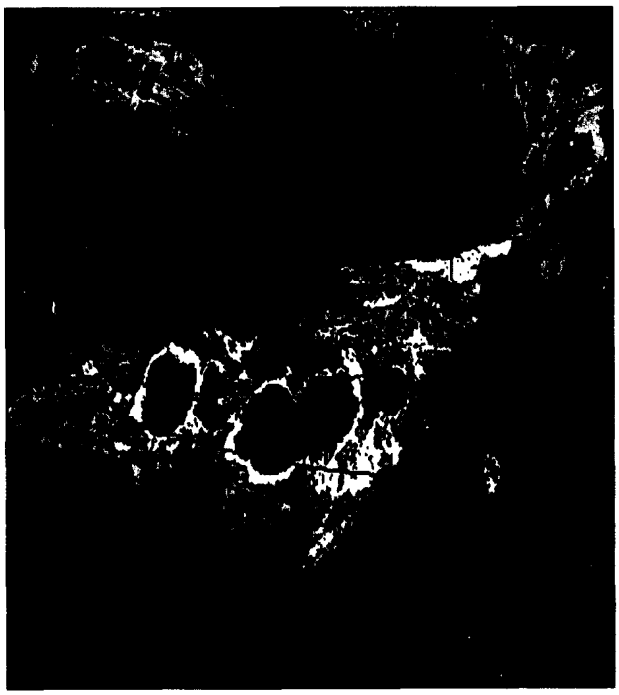

Fig.8 The enhanced infrared imagery of GOES-9 satellite at 0000 UTC 7 June 2003. The bolded dash line represents the position of surface front.

The lowest elevation (0.5°) of plan position indicator (PPI) showed that the initiation of LEWP was characterized by multi-cellar structure (fig. 9) located from 100 to 250 km off southwestern coast of Taiwan at

0003 UTC 7 June 2003. Later on these cells organized into a QLCS with slight curvature. By 0203 UTC, two intense echoes evolved into bow-shaped systems, which were denoted by A and B, respectively, and propagated toward the east at a speed of 15 ms^{-1}. According to the category of initial bow echoes defined by Klimowski et al. (2004), the system A and B developed from the merger of weakly organized (WO) cells evidently. System A exhibited rather asymmetric at its mature stage. It sustained for only 1 hour and dissipated after moving inland. System B also evolved into a comma echo after an hour. Meanwhile a convective cell connected with the southern end of system B had a bow-shaped leading edge, which was denoted as system C. The system B and C constructed a well pronounced LEWP while propagating to southeastern Taiwan. Both systems weakened until around 0600 UTC; however, remnants of MCS still existed located around 120 km off southernmost point of Taiwan. Consequently, the life time of system B and C was over 6 hours, yet system A only sustained less than 2 hours.

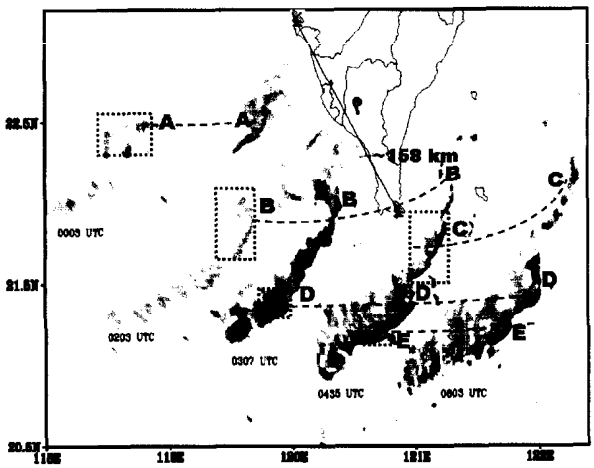

Fig.9 The reflectivity of elevation of 0.5 degree from RCCG radar (0003 and 0203 UTC) and RCKT radar (0307, 0435 and 0603). The shaded area stand for echoes of 30, 40 and 45 dBZ, respectively. Symbol Λrepresents the position of Pingtung sounding station.

4. Mesoscale feature

The analysis of reflectivity demonstrated that systems within LEWP attributed a comparable evolution with bow echoes, which used to be observed over the plain in the central United States. This inducts a useful conceptual model to investigate the mesoscale characteristics of such bow-shaped systems.

A long, narrow weak echo region with V-shaped could be determined behind system B by 0204 UTC 7 June 2003 (fig. 10a). The concave region was obvious below 4 km in height associated with intense inbound Doppler velocity of ground relative speed over 24 ms^{-1}, indicating that a flow was traveling from the rear to the front of the system. It firmly existed while the system kept on moving eastward (fig. 8 c, d). Such features characterized as weak echo channel, rear-inflow notch and rear-inflow jet, respectively, which had been specified from being documented bow echo studies. Accordingly, the estimated intensity of current RIJ was less than 30 ms^{-1}, which is quite similar to an observation in the vicinity of Hawaii (~26 ms^{-1}, Businger et al. 1998). However, it was somehow less than that of RIJ in midlatitude that was typically over 40 ms^{-1}.

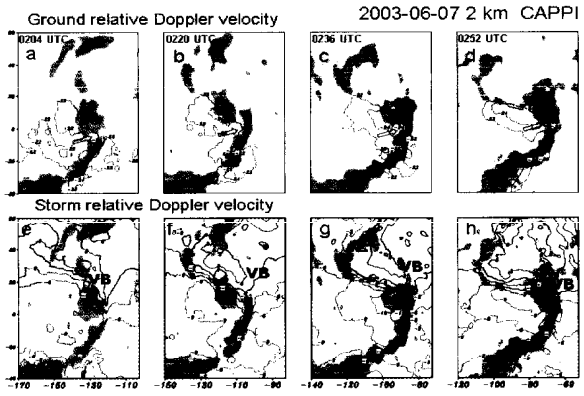

Fig.10 CAPPIs performed by implementing Kenting radar data for 0204, 0220, 0236 and 0252 UTC 7 June 2003,respectively, at 2 km level. Doppler wind field in (a) to (d) represent ground relative velocity, and (e) to (h) represent storm relative velocity. 0236 and (d) 0252 UTC on 7 June 2003. The Shaded areas represent reflectivity of 30, 35, 40 and 45 dBZ. Contours show the intensity of Doppler velocity. Arrows point out the existence of rear-inflow notch. The X and Y axis are the east-west and south-north distances far from radar site.

While the bow echo propagated to the east side of RCKT radar site, it was easy to recognize that the RIJ is a northwesterly by the signature of Doppler velocity. The analysis of cross section was feasible to understand vertical characteristics of bow echo B1 and B2. By 0444 UTC, the vertical structure of bow echo B1 (fig. 9b) exhibited a slight slantwise toward its moving direction. The positive Doppler velocity behind the leading edge, which was represented as RIJ, extended to 5 km of altitude and decelerated within the convection. On the contrary, the leading edge of bow echo B2 (fig. 9b) was upright in vertical, and the depth of RIJ was 4 km above ground level so that lifted the front-to-rear flow up to 5 km in height. Therefore, a transition between negative and positive Doppler velocity existed between the altitude of 4 and 5 km, which was similar to MARC. The intense reflectivity (> 30 dBZ) of both bow echoes extended to almost 9 km in height. As a result, the vertical structure of bow echo B2 resembled that of classical (midlatitude) bow echoes. Bow echo B1 exhibited a partially different structure in vertical, although the diverse vertical profile of Doppler velocity might be due to azimuthal projection of real wind field.

The RIJ was described as a drier and colder air with high momentum by documented researches (Smull and Houze 1985, 1987). Therefore the current would generate a long thin channel of weak echo behind the convective line while penetrating into concentrated echo. The Heng-chun and Lan-yu surface weather observational station provided surface data of 1 minute interval for each meteorological factor which was feasible to analyze the characteristics of RIJ in present case, since the northern head of bow echo B passed Heng-chun station (fig. 10a) between 0348 and 0356 UTC, as well as passed Lan-yu between 0448 and 0500 UTC. During the passage of bow echo B over Heng-chun, the air temperature dropped for 3 °C, associated with see level pressure jump of 0.7 hPa. The information thus indicated that a cool pool existed behind bow echo B, so that RIJ was attributed to a colder flow. However, the difference between air temperature and dew point was quite the same as before and after bow echo B passage, which implied that the RIJ was not a drier air. At Lan-yu (fig. 10b) the

passage of bow echo B did not produce a severe variation onto temperature and sea level pressure as at Heng-chun, even the tendency of dew point superimposed on that of air temperature. The results suggested that the drier characteristic of RIJ was not well pronounced, probably due to the adjustment of moisture driven from sea surface.

5. Mesovortices

The line echo wave pattern was composed of several bow echoes of various scales. In this study the bow echo B was the principal segment of whole LEWP. A cyclonic shear of Doppler velocity at the northern end of bow echo B was remarkable by 0204 UTC (fig. 11a) and strengthened gradually, illustrating an implicit signature of cyclonic vortex. It could also be verified while propagating into the coverage of RCCG radar, revealing a velocity couplet on the southern side of radar sire (fig. 12). The coverage of RCCG radar was only 120 km in radius so that data collected from RCKT radar was more available. Since the intersecting angle between moving direction of bow echo B (toward east with speed of about 14 ms^{-1}) and radar beam was pretty small in the area, the prominent component of Doppler velocities responded system moving speed. Therefore, a couplet did not show up and a shear replaced. In order to deduce the couplet of Doppler velocity within the region, the system moving speed needed be eliminated. The distinct cyclonic couplet on the northern end of bow echo B was denoted as vortex VB1 (fig. 11). Its mean vertical vorticity of the vortex was approximately estimated from average of maximum negative of positive radial velocity and distance between both peak values. And the method that analyzed accompanying mesovortices referred to Atkins et al. (2004).

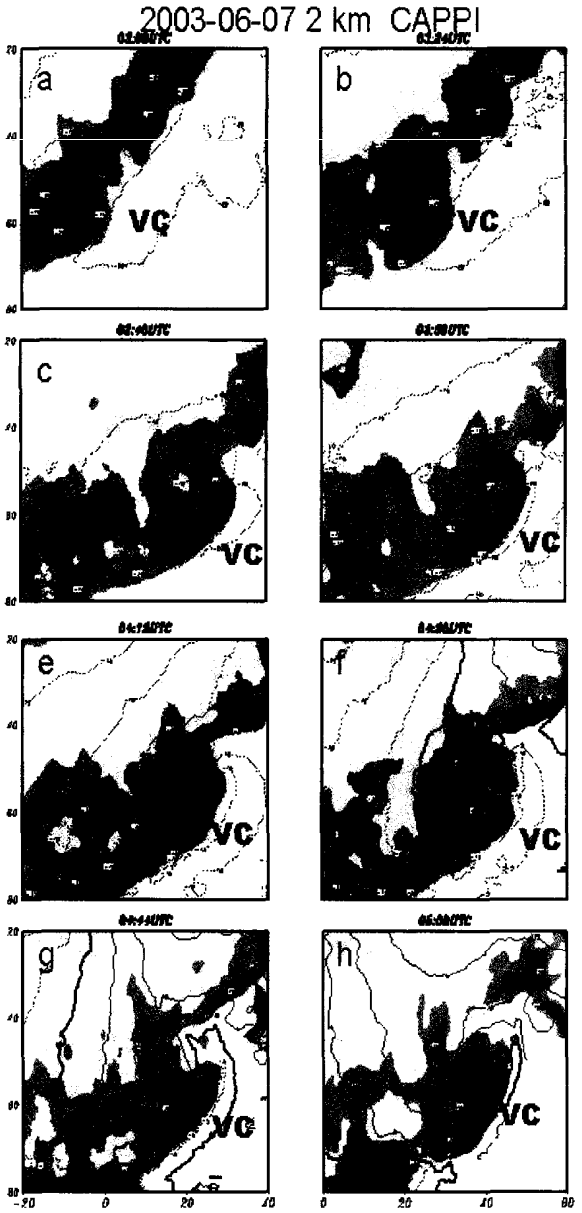

Fig.11 CAPPIs performed by implementing Kenting radar data for (a) 0308, (b) 0324, (c) 0340, (d) 0356, (e) 0412, (f) 0428,(g) 0440 and (h) 0500 UTC 7 June 2003, respectively, at 2 km level.. The Shaded areas represent reflectivity of 30, 35, 40 and 45 dBZ. Contours show the intensity of Doppler velocity. The X and Y axis are the east-west and south-north distances far from radar site.

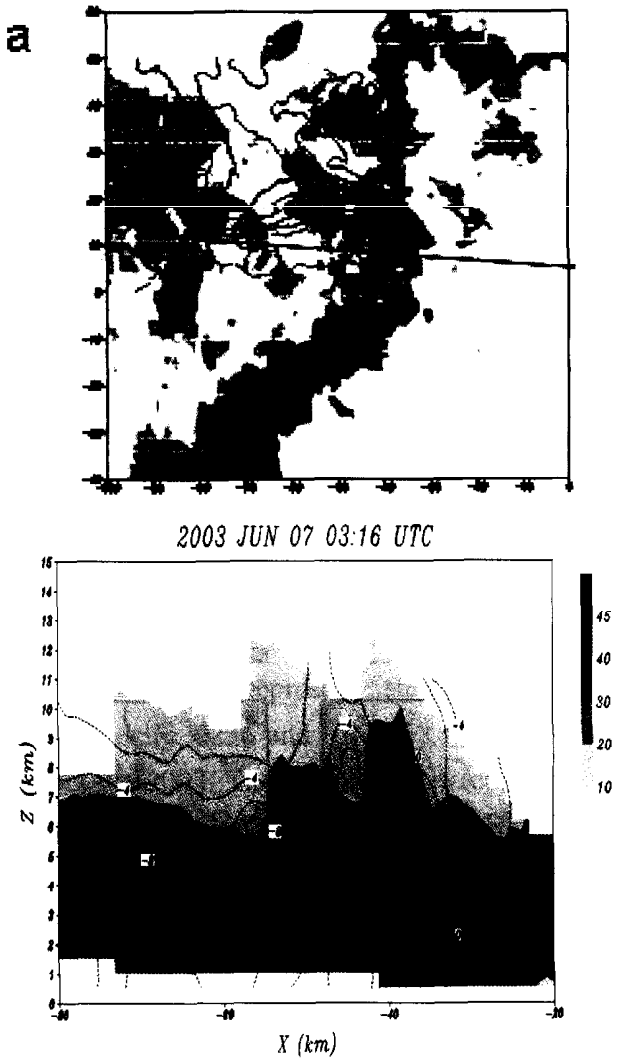

Fig.12 Vertical cross sections at 0316 UTC 7 June 2003. The X axis represents distance far from radar site. The Shaded areas represent reflectivity and contours illustrate the intensity of Doppler velocity.

The vertical vorticity of vortex VB1 strengthened between 4 and 6 km in height from 0204 and 0300 UTC (fig. 13), with maximum magnitude around 1.5×10^{-3} s^{-1}. There were two peak values appeared at the period from 0220 to 0230 UTC, and from 0250 to 0300 UTC. Considering the zero value of radial velocity illustrated in CAPPI, the zero contours inside the vortex VB1 exhibited considerate curved at level of 2 km by 0220 and 0228 UTC, in which suggested that smaller scale disturbances developed in it. In addition to the cyclonic vortex, there was no couplet which resembled an anticyclonic vortex on the southern end of the bow echo B, implying lack of the anticyclonic portion of bookend vortices. The conclusion offered an inference that cyclonic vortex VB1 was the only dominated vortex associated with bow echo B.

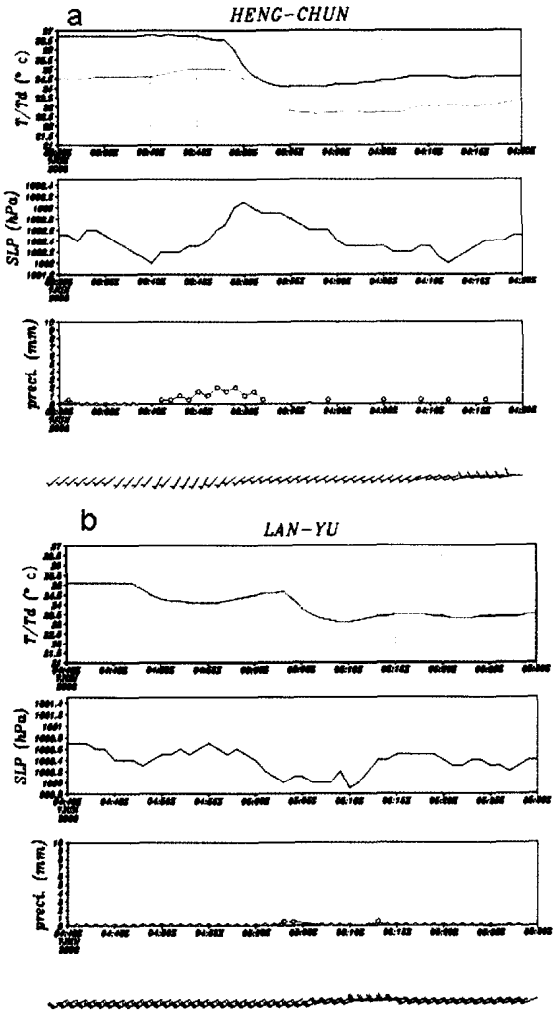

Fig.13 Surface observation of temperature, dew point, sea level pressure, accumulated precipitation and wind field by 1 minute interval from (a) Heng-Chun and (b) Lan-Yu station.

As bow echo B2 was evolved from a convective cell, gradients of Doppler speed along the leading edge of the bow echo enhanced (fig. 14) into a significant cyclonic shear. After 0412 UTC (fig. 14c) a couplet of Doppler velocity appeared on the northern side of bow echo B2, which was denoted as vortex VB2. Its mean vorticity estimated by the same method as mentioned previously revealed temporal and vertical differences from vortex VB1. Since the couplet signature of vortex VB2 was distinctive below 4 km in height, the discussion on vertical distribution of vorticity was only focused on the low level (less than 4 km) (fig.15). The vorticity of vortex VB2 below 2 km level strengthened from 0324 to 0340 UTC, coinciding with bowing of bow echo B2. Between 0412 and 0420 UTC the vorticity intensified with maximum magnitude over 2.5 $\times 10^{-3}$ s^{-1}. The bowing of bow echo B2 was clearly delineated meanwhile. It was evident that the development of vorticity corresponded to that of bow echo B2.

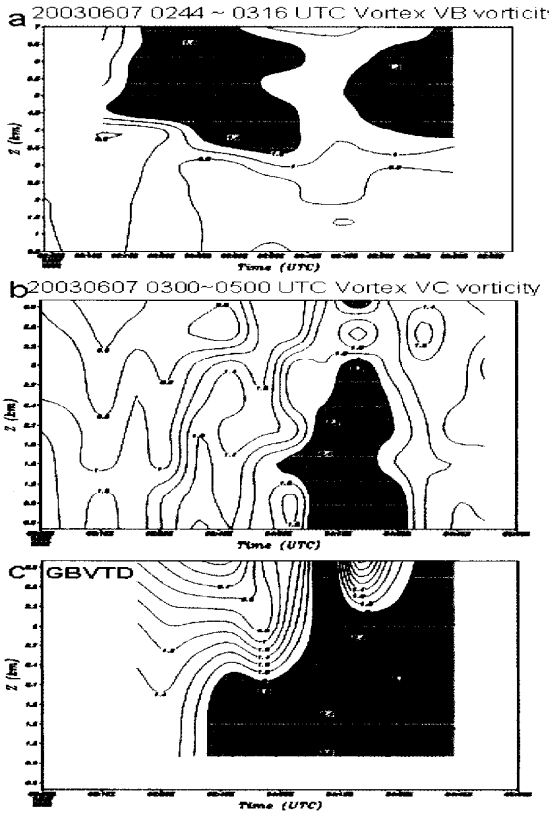

Fig.14 The time-height sequences of mean vertical vorticity. (a) vortex VB, (b) vortex VC and (c) estimation from GBVTD derived wind field for vortex VC. The unit is 10-3 s-1.

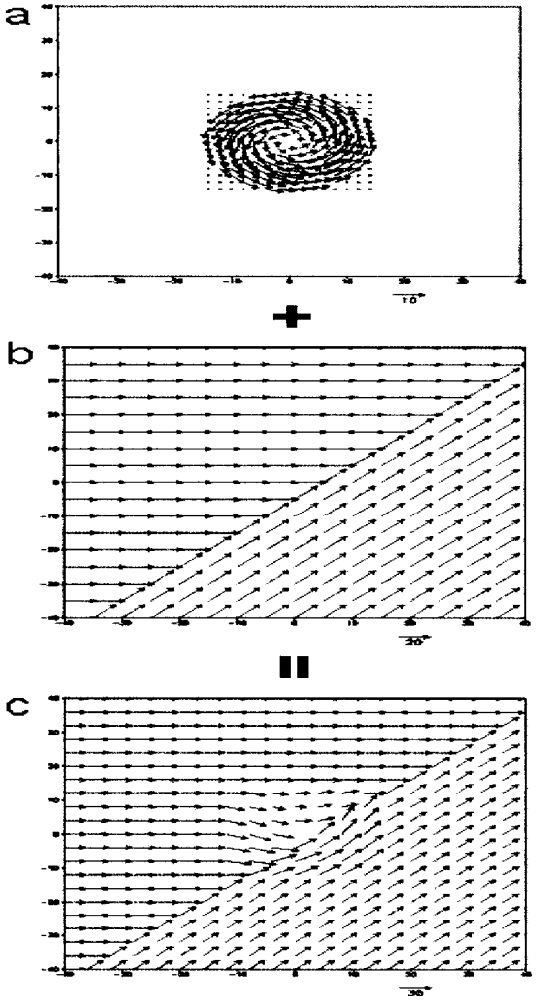

Fig.15 The simulation of ideal flow pattern. (a) a Rankin vortex, (b) westerly and southwesterly divided by a diagonal and (c) combination of the ideal wind.

The radial component of vorticity was also estimated by only applying Doppler velocity (figures not shown), though it was lack of observation of cross beam component all the time. The vorticity along the leading edge of bow echo B2 was intense and increased

Comparing with the maximum vorticity of vortices associated with midlatitude bow-echoes, Lee et al. (1992) estimated the vorticity of cyclonic vortex which observed in Colorado was approximate 5×10^{-3} s^{-1}. The vorticity assessed from numerical model by Weisman and Trapp (2003) was 2×10^{-2} s^{-1}. Therefore, the vorticity of cyclonic vortex, which developed in midlatitude, estimated by either observation or numerical model was larger than that of the present case study accordingly.

6. Summary

The observation of a MCS, which possessed a region from southern Taiwan Strait to southern Taiwan area on 7 June 2003, revealed a bow-shaped leading edge through radar reflectivity data. Both Kenting and Chiku Doppler weather radar provided prominent data to elucidate the evolution of the bow echo systems. The summarized conclusions of the study are as following:

1. The CAPE value for a developing LEWP in this study is over 2000 J kg-1, which is similar to that for a midlatitude counterpart. However, the strength of vertical wind shear is 15 ms-1 below 700 hPa which is also one of the suitable conditions for the development of a tropical squall line systems.

2. The mesoscale features of typical bow echoes, such as weak echo channel, rear-inflow notch and rear-inflow jet, can also be

following time. Its maximum reached to 8×10^{-3} s^{-1} by 0420 UTC, suggesting that smaller scale disturbances associated with the leading line. However, to verify the existence of such small systems was difficult until an intensive field experiment is proposed.

determined in a subtropical bow echo. The intensity of RIJ identified in the case study, however, is weaker (less than 30 ms-1) comparing with the RIJ associated with typical bow echoes (over 40 ms-1). It is only comparable to the RIJ observed in the vicinity of Hawaii (~26 ms-1). Besides, the RIJ is characterized as a colder but moister air. The modification of moisture driven from sea surface may play a significant role for its explicit thermodynamic characteristic.

3. Two mesocyclone signatures were located on the northern side of bow echoes, with magnitude of vorticity between 1.5 ×10-3 and 2.5 ×10-3 s-1. The amount was less than that observed in midlatitude. The bookend vortices were not pronounced, since the anticyclonic signature did not exist or was not detected by RCKT radar.

From the perspective of civilian forecasting, the northern portion of bow echo B brought considerate precipitation while passing southern part of Taiwan between 0300 and 0400 UTC. The accumulated rainfall in Heng-chun station was 12 mm only during passage of bow echo B (from 0342 to 0354 UTC, fig. 10a), indicating that this bow echo was a severe precipitating system. The wind direction varied from southwest to west smoothly, with wind speed increasing only 2.5 ms-1 (from 2.5 to 5 ms-1) which was far from the criterion of downburst. Actually, to define the existence of downburst was hard since the

apex of bow echo B did not pass through any surface observational station. Yet the orientation of runway at Heng-chun airport is north-south, a slight variation of wind direction and speed before and after passage of a bow echo will produce a remarkable cross wind. This information is significant for the aeronautical forecaster.

The new Doppler radar network located on southern Taiwan area is available to recognize the mesoscale characteristics of bow echoes over southeastern Asian ocean and the signatures of associated mesovortices, which have never been documented yet. The future attempt is to synthesize dual-Doppler wind from RCCG and RCKT radar in order to understand the kinematic and dynamical field of subtropical bow echoes.

Acknowledgement

We especially appreciate Central Weather Bureau for providing weather radar data. The computing facilities for this research are supported by Chung Cheng Institute of Technology and the National Center for Atmospheric Research, USA.

References

Atkins, N. T., J. M. Arnott, R. W. Przybylinski, R. A. Wolf and B. D. Ketcham, 2004: Vortex Structure and Evolution within Bow Echoes. Part I: Single-Doppler and Damage Analysis of the 29 June 1998 Derecho. *Mon. Wea. Rev.*, **132**, 2224 -2242.

Barnes, S. L, 1980: Report on a meeting to establish a common Doppler radar data exchange format.Bull. *Amer. Meteor. Soc.*, **61**, 1401-1404.

Burgess, D. W., and B. F. Smull, 1990: Doppler radar observations of a bow echo associated with a long-track severe windstorm. Preprints, *16th Conf. on Severe Local Storms*,Kananaskis Park, AB, Canada, Amer. Meteor. Soc., 203–208.

Businger, S., T. Birchard Jr., K. Kodama, P. A. Jendrowski, and J. J. Wang, 1998: A bow echo and severe weather associated with a Kona Low in Hawaii. *Wea. Forecasting*, **13,** 576–591.

Davis, C., N. Atkins, D. Bartels, L. Bosart, M. Coniglio, G. Bryan, W. Cotton, D. Dowell, B. Jewett, R. Johns, D. Jorgensen, J. Knievel, K. Knupp, W.-C. Lee, G. Mcfarquhar, J. Moore, R. Przybylinski, R. Rauber, B. Smull, R. Trapp, S. Trier, R. Wakimoto, M. Weisman and C. Ziegler, 2004: The Bow Echo and MCV Experiment: Observations and Opportunities. *Bulletin of the American Meteorological Society*: **85,** 1075-1093.

Fujita, T. T., 1978: Manual of downburst identification for project Nimrod. Satellite and Mesometeorology Research Paper 156, Dept. of Geophysical Sciences, University of Chicago, 104 pp. [NTIS PB-286048.]

Fujita T. T., 1981: Tornadoes and Downbursts in the Context of Generalized Planetary Scales. *J. Atmos. Sci* , **38**, 1511–1534.

Jorgensen, D. P., and B. F. Smull, 1993: Mesovortex circulations seen by airborne Doppler radar within a bow-echo mesoscale convective system. *Bull. Amer. Meteor. Soc.*, **74,** 2146–2157.

Jorgensen, D. P., M. A. LeMone and S. B. Trier, 1997: Structure and evolution of the 22 February 1993 TOGA COARE squall line, Aircraft observations of Precipitation, Circulation, and Surface Energy Fluxes. *J. Atmos. Sci.*, **54**, 1961–1985.

Johns, R. H., and W. D. Hirt, 1987: Derechos: Widespread convectively induced wind-storms. *Wea. Forecasting*, **2,** 32–49.

Klimowski, B. A., M. R. Hjelmfelt and M. J. Bunkers. 2004: Radar Observations of the Early Evolution of Bow Echoes. *Wea Forecasting*, **19**, 727–734.

Lee, W.-C., R. M. Wakimoto, R. E. Carbone. 1992: The evolution and structure of a "bow–echo-microburst" event. Part II: The Bow Echo. *Mon. Wea. Rev.*, **120**, 2211–2225

Przybylinski, R. W., 1995: The bow echo. Observations, numerical simulations, and severe weather detection methods. *Wea. Forecasting,* **10,** 203–218.

Przybylinski, R. W., and W. J. Gery, 1983: The reliability of the bow echo as an important severe weather signature. Preprints, *13th Conf. on Severe Local Storms,* Tulsa, OK, Amer. Meteor. Soc., 270–273.

Przybylinski, R. W., and D. M. DeCaire, 1985: Radar signatures associated with the derecho, a type of mesoscale convective system. Preprints, *14th Conf. on Severe Local Storms,* Indianapolis, IN, Amer. Meteor. Soc., 228–231.